

# DYNAMICS AND INSTABILITIES OF NUCLEAR FERMI LIQUID

V.M.Kolomietz

*Institute for Nuclear Research, Prosp. Nauki 47, 252028 Kiev, Ukraine*

## Abstract

The kinetic theory of Fermi liquid is applied to finite nuclei. The nuclear collective dynamics is treated in terms of the observable variables: particle density, current density, pressure etc. The relaxation processes and the development of instabilities in nuclear Fermi-liquid drop are strongly influenced by the Fermi-surface distortion effects.

PACS numbers: 21.60.-n,21.60.Ev,24.30Cz

arXiv:nucl-th/9809047v1 15 Sep 1998

Typeset using REVTeX

## I. INTRODUCTION. NUCLEAR FERMI-LIQUID DROP MODEL

Dynamics and dissipative properties of nuclear Fermi liquid depend in many aspects on the dynamic distortion of the Fermi surface in the momentum space. It is well-known that taking into account this distortion allows the description of a new class of phenomena, most famous of which are giant multipole resonances. Furthermore, scattering of particles from the distorted Fermi surface leads to relaxation of collective motion and gives rise to fluid viscosity [1]. We point out that the development of instability in nuclear processes like binary fission or multifragmentation in HI-reactions also depends on dynamic effects such as the dynamic Fermi-surface distortion.

A convenient way to introduce the Fermi-liquid effects into the nuclear many body problem is to start from the kinetic equation for the phase space distribution function  $f(\vec{r}, \vec{p}, t)$ . The kinetic equation can then be transformed identically to a set (infinite) of equations for the moments of  $f(\vec{r}, \vec{p}, t)$  in  $\vec{p}$ -space, namely, local single-particle density  $\rho$ , the velocity field  $\vec{u}$ , the pressure tensor  $\pi_{\alpha\beta}$ , etc., see [1]. In case of small variations of the particle density,  $\delta\rho$ , the first order moment of the kinetic equation has the form of Euler-Navier-Stokes equation and is given by [2]

$$m\rho_{eq}\frac{\partial}{\partial t}u_\alpha + \rho_{eq}\frac{\partial}{\partial r_\alpha}\left(\frac{\delta^2\mathcal{E}}{\delta\rho^2}\right)_{eq}\delta\rho + \frac{\partial}{\partial r_\nu}\pi_{\nu\alpha} = 0. \quad (1)$$

The internal energy density  $\mathcal{E}$  in Eq. (1) contains both kinetic  $\mathcal{E}_{kin}$  and potential  $\mathcal{E}_{pot}$  energy densities:  $\mathcal{E} = \mathcal{E}_{kin} + \mathcal{E}_{pot}$ . The pressure tensor  $\pi_{\alpha\nu}$  depends on the Fermi-surface distortion effect. In general case, tensor  $\pi_{\alpha\nu}$  also includes the viscosity tensor which is derived by the collision integral.

Eq. (1) is not closed because it contains the pressure tensor  $\pi_{\alpha\beta}$  given by the second order moment of the distribution function  $f(\vec{r}, \vec{p}, t)$ . We will follow the nuclear fluid dynamic approach [3–5] and take into account dynamic Fermi-surface distortions up to the multipolarity of  $l = 2$ . Assuming a periodic in time eigenvibrations with the eigenfrequency  $\omega = \omega_0 + i\Gamma/2\hbar$ , where  $\omega_0$  and  $\Gamma$  are real, and a separable form of the velocity field,

$\vec{u}(\vec{r}, t) = \beta(t)\vec{v}(\vec{r})$ , with  $\beta(t) \sim e^{-i\omega t}$ , Eq. (1) is reduced to the equation of motion for the macroscopic variable  $\beta(t)$  with the following secular equation

$$-\omega^2 B + (C^{(LD)} + C'(\omega)) - i\omega\gamma(\omega) = 0. \quad (2)$$

Here,  $B$  and  $C^{(LD)}$  are the mass coefficient and the stiffness coefficient in the traditional liquid drop model (LDM) [6] respectively. The additional contribution from  $C'(\omega)$  to the stiffness coefficient and the dissipative term  $\gamma(\omega)$  depend on the relaxation time  $\tau$  and are given by

$$C'(\omega) = \int d\vec{r} P_{eq} \frac{(\omega_0\tau)^2}{1 + (\omega_0\tau)^2} \left( \frac{\partial v_\alpha}{\partial r_\nu} + \frac{\partial v_\nu}{\partial r_\alpha} - \frac{2}{3} \delta_{\alpha\nu} \frac{\partial v_\lambda}{\partial r_\lambda} \right) \frac{\partial v_\alpha}{\partial r_\nu} \quad (3)$$

and

$$\gamma(\omega) = \int d\vec{r} P_{eq} \frac{\tau}{1 + (\omega_0\tau)^2} \left( \frac{\partial v_\alpha}{\partial r_\nu} + \frac{\partial v_\nu}{\partial r_\alpha} - \frac{2}{3} \delta_{\alpha\nu} \frac{\partial v_\lambda}{\partial r_\lambda} \right) \frac{\partial v_\alpha}{\partial r_\nu}, \quad (4)$$

where  $P_{eq}$  is the equilibrium pressure of the Fermi gas. The additional contribution from  $C'(\omega)$  to the stiffness coefficient in Eq. (2) is absent in the LDM, i.e. in the liquid drop limit  $\omega\tau \rightarrow 0$ , and represents the influence of the dynamic Fermi-surface distortion on the conservative forces in the Fermi system. Finally, the dissipative term  $\gamma(\omega)$  appears due to the interparticle scattering from the distorted Fermi surface.

In general, both,  $C'(\omega)$  and  $\gamma(\omega)$  depend implicitly on the temperature,  $T$ , via the dependence of the relaxation time  $\tau$  and of  $P_{eq}$  on  $T$ . In cold nuclei, in the zero-sound limit  $\omega\tau \rightarrow \infty$ , the main contribution to the stiffness coefficient in Eq. (2) is due to the Fermi-surface distortion effect given by  $C'(\omega)$ . In Fig. 1, this effect is shown in a transparent way for isoscalar quadrupole excitations. As it is seen from this figure, the Fermi-surface distortion effect leads to a significant upward shift of the energy of vibrational states to locate it in the region of the quadrupole giant resonance (solid line).

## II. GIANT MONOPOLE RESONANCE AND NUCLEAR INCOMPRESSIBILITY

We will discuss the Fermi-surface distortion effect in more detail for the case of isoscalar giant monopole resonances (ISGMR). This particular case is important for understanding

the nature of nuclear incompressibility. We will consider below the model for a Fermi-liquid drop having a sharp surface of the equilibrium radius  $R_0$  and the bulk density  $\rho_0$ .

The particle density variation  $\delta\rho$  is then given by

$$\delta\rho(r, t) = \eta(r, t) \rho_0 \theta(R_0 - r) + q(t) \rho_0 R_0 \delta(R_0 - r), \quad (5)$$

where the unknown functions  $\eta(r, t)$  and  $q(t)$  are related to each other by the particle number conservation and the bulk density parameter  $\eta(r, t)$  is found from the equation of motion derived by Eq. (1). Namely,

$$m \frac{\partial^2}{\partial t^2} \eta = \frac{1}{9} K' \nabla^2 \eta \quad \text{with} \quad K' = K + K_\mu. \quad (6)$$

Here  $K$  is the *static* incompressibility

$$K = R^2 \left. \frac{\delta^2 E/A}{\delta R^2} \right|_{R=R_0}. \quad (7)$$

The additional contribution  $K_\mu$  to the incompressibility  $K'$  in Eq. (6) is due to the *dynamic* Fermi-surface distortion effect [3,7]. The value of  $K_\mu$  depends on the Landau scattering amplitude  $F_0$ . In nuclear case,  $F_0 \sim 0$ , one has  $K_\mu \approx 2K$ .

An essential property of a finite liquid drop having a free surface is that the motion of the surface should be consistent with the motion of the liquid inside the drop. This can be achieved by imposing a boundary condition for the compensation of the compressional pressure  $\pi_{rr}$  at the liquid surface by the pressure generated by the surface tension forces  $\delta P_\sigma$ . Finally, the eigenenergies in Eq. (6) are given by

$$\hbar \omega_n = \sqrt{\frac{\hbar^2 K'}{9 m R_0^2}} x_n, \quad (8)$$

where  $x_n = k_n R_0$  are derived from the following boundary condition:

$$x_n j_0(x_n) - (f_\sigma + f_\mu) j_1(x_n) = 0. \quad (9)$$

Here the coefficients  $f_\sigma$  and  $f_\mu$  are related to the surface tension and the Fermi-surface distortion respectively and are given by

$$f_\sigma = \frac{18\sigma}{\rho_0 R_0 K'}, \quad f_\mu = \frac{3K_\mu}{K'}. \quad (10)$$

In the general case of Fermi-liquid drop with  $f_\mu \neq 0$ , the eigenfrequency  $\omega_n$  given in Eq. (8) is renormalized due to two contributions associated with the Fermi-surface distortion: 1) the direct change of the sound velocity, i.e. in Eq. (8)  $K'$  appears instead of  $K$ ; 2) the change of the roots  $x_n$  of the secular equation (9) due to additional contribution from  $f_\mu \neq 0$  in Eq. (9). These two effects work in opposite directions:  $K'$  increases  $\omega_n$  while  $f_\mu$  in Eq. (9) decreases it. Both values of  $K'$  and  $x_n$  in Eq. (8) depend on the Landau scattering amplitude  $F_0$ . In the limit of zero- to first sound transition at  $F_0 \gg 1$ , one has  $f_\mu \rightarrow 0$  and the solution of Eqs. (9) and (8) is close to the one obtained in LDM. However, for realistic nuclear forces  $F_0 \sim 0$ , the general expressions (9)-(8) with  $f_\mu \neq 0$  have to be used.

In Fig. 2 we plotted the eigenenergy,  $E_{0+}$ , of the lowest monopole mode ( $n = 1$ ) given by Eqs. (8) and (9) as a function of mass number  $A$ . The dashed line shows the result for  $E_{0+}$  from Eq. (8) where  $K'$  was replaced by  $K_{LDM} = 190 \text{ MeV}$  and boundary condition (9) with  $f_\mu = f_\sigma = 0$  was used. The solid line shows the result of FLDM calculations. We adopted the following expression for  $K$  [8]  $K = K_\infty + K_\sigma A^{-1/3}$  with  $K_\infty = 220 \text{ MeV}$  and  $K_\sigma = -440 \text{ MeV}$  and for  $\rho_0 = 0.17 \text{ fm}^{-3}$ ,  $\epsilon_F = 40 \text{ MeV}$ ,  $r_0 = 1.12 \text{ fm}$  and  $\sigma = 1.2 \text{ MeV/fm}^2$ . So, in spite of strong renormalization of nuclear incompressibility due to the Fermi-surface distortion effect, the energy of the giant monopole resonance  $E_{0+}$  in the Fermi-liquid drop is located close to the one in the traditional LDM [6] where the Fermi-surface distortion effects are absent. The compensation of the Fermi-surface distortion effect in nuclear incompressibility  $K'$  due to the consistent account of the same effect in the boundary condition (9) is essential for the lowest mode ( $n = 1$ ) only. The above mentioned compensation is rather small for the highest modes with  $n \geq 2$ . In particular, the eigenenergy of the double (overtone) giant monopole resonance  $E_{0_2^+}$  (in contrast to  $E_{0+}$ ) has a significant upward shift with respect to  $E_{0_2^+}^{LDM} \approx 2 E_{0+}$  given by the traditional liquid drop model.

### III. COLLISIONAL RELAXATION ON THE DEFORMED FERMI SURFACE

The relaxation of nuclear collective motion toward thermal equilibrium has been described in great detail within the framework of the kinetic theory, taking into account the collision integral  $\delta St(\vec{r}, \vec{p}, t)$  [3,5,7,9–11]. The collision integral  $\delta St(\vec{r}, \vec{p}, t)$  depends on the equilibrium distribution function,  $f_{eq}(\vec{r}, \vec{p})$ . In case of a finite Fermi system, the equilibrium distribution function,  $f_{eq}(\vec{r}, \vec{p})$ , contains both the diffusive layer and oscillations in  $\vec{p}$ -space which are caused by particle reflections at the potential surface. Both of them depend on the distance  $r$ . This fact also leads to the  $r$ -dependence of the collisional relaxation time,  $\tau_2(r, \omega)$ , given by

$$1/\tau_2(r, \omega) = - \int d\vec{p} p^2 Y_{20} \delta St / \int d\vec{p} p^2 Y_{20} \delta f. \quad (11)$$

The  $\omega$ -dependence of  $\tau_2(r, \omega)$  is due to the memory effects in the collision integral [7].

The evaluation of the collisional relaxation time  $\tau_2(r, \omega)$  in a finite Fermi system requires additional accuracy. The diffusive layer in the equilibrium distribution function in momentum space can lead to a spurious effect in non-zero gain- and loss fluxes of the probability in the ground state of the Fermi system. However, it can be shown, see Ref. [11], that the general condition for the disappearance of both above mentioned fluxes is reached due to the occurrence of quantum oscillations in the equilibrium distribution function  $f_{eq}(\vec{r}, \vec{p})$  in momentum space. The  $r$ -dependent diffusive tail of the distribution function in momentum space leads to an increase of the collisional damping of the collective motion in the surface region of a nucleus and thus to an increase of the isoscalar giant quadrupole resonance (GQR) width. However, this increase is strongly reduced due to the above mentioned oscillations of the equilibrium distribution functions appearing in the collision integral. As a result, the collisional width of the isoscalar GQR does not exceed 30-50% of the experimental value and agrees with the estimates of the width where the sharp Thomas-Fermi distribution function is used [11].

In the case of heated nuclei, both temperature and memory effects have to be taken into

account in the collision integral. For frequencies small compared to the Fermi energy, one finds [7,12]:

$$1/\tau_2 = [1 + (\hbar\omega_0/2\pi T)^2]/\tilde{\tau}_2, \quad (12)$$

which is valid for  $T, \hbar\omega_0 \ll \epsilon_F$  and when sharp Thomas-Fermi distribution for  $f_{eq}(\vec{r}, \vec{p})$  is assumed. The magnitude of  $\tilde{\tau}_2$  can be given in the following general form at low temperatures  $T \ll \epsilon_F$  [5]

$$\tilde{\tau}_2(T)/\hbar = \alpha^{(\pm)}T^{-2}, \quad (13)$$

where the quantity  $\alpha^{(+)}$  is for the isoscalar mode and  $\alpha^{(-)}$  is for the isovector mode:  $\alpha^{(+)} = 9.2 \text{ MeV}$  and  $\alpha^{(-)} = 4.6 \text{ MeV}$  [10].

In general, there are several contributions to the relaxation time  $\tau$ . The main contribution  $\tau_2$  arises from the above discussed interparticle collisions and the other from collisions of nucleons with the moving nuclear surface (one-body dissipation with relaxation time  $\tau_1$ ). We will also include the contribution from particle emission with relaxation time  $\tau_\uparrow$ . Thus,

$$1/\tau = 1/\tau_1 + 1/\tau_2 + 1/\tau_\uparrow. \quad (14)$$

Introduction of the one-body dissipation reflects the peculiarities of our consideration, namely, restricting Fermi-surface distortions to the multipolarity  $l \leq 2$  does not allow us to take into consideration Landau damping (fragmentation width).

The total width,  $\Gamma$ , of a collective state can be derived from Eq. (4) with  $\tau_2$  replaced by the total relaxation time  $\tau$  from Eq. (14). Assuming sharp nuclear surface, the total width  $\Gamma$  is reduced to the following form, see Ref. [10],

$$\Gamma \approx 2x\hbar\omega_0 \frac{\omega_0\tau}{1+x(\omega_0\tau)^2}, \quad (15)$$

where  $x \approx (1/6)(v_F/u_1)^2$  and  $u_1$  is the first sound velocity in nuclear matter. We want to note that the total intrinsic width given by Eq. (15) has a bell-shaped form as a function of  $y = \omega_0\tau$ . The width  $\Gamma$  is peaked around  $y \equiv y_0 = x^{-1/2}$  and the maximum value of  $\Gamma$

is  $\Gamma_{max} = \hbar\omega_0 x^{1/2}$ . It is easy to see that  $y_0$  represents the crossing point of both curves  $\Gamma^{(0)}(y) \sim 1/\tau$  (zero sound regime) and  $\Gamma^{(1)}(y) \sim \tau$  (first sound regime). Due to this fact the condition

$$\omega_0\tau \equiv y_0 = (\omega_0\tau)_0 = x^{-1/2} \quad (16)$$

can be used as the condition for the transition from long to short relaxation time regimes. The magnitude of the intrinsic width  $\Gamma$  decreases when the parameter  $\omega_0\tau$  exceeds  $y_0$ . We have  $y_0 = 2.28$  for the isovector GDR at the realistic value of  $x = 0.19$ . Such a value of  $\omega_0\tau$  can be reached at the temperature  $T \equiv T_{tr} \approx 4.5 \text{ MeV}$ , see Eq. (12). If the relation (16) with  $x = 1$  and  $\tau = \tau_2$  is used as the condition for transition between different regimes of sound wave propagation then the transition between both regimes occurs at the higher temperature  $T_{tr} \approx 10 \text{ MeV}$ . In Fig. 3 we show the intrinsic width of the giant dipole resonance (GDR) in the nucleus  $^{112}\text{Sn}$ . As it is seen from Fig. 3, the expression (15) (solid line) leads to a smoother behaviour of the total intrinsic width with increasing excitation energy as compared to the prediction of the zero-sound regime given by the following condition:  $\Gamma \approx 2\hbar/\tau = \Gamma_1 + \Gamma_2 + \Gamma_\uparrow$  with  $\Gamma_1 = 2\hbar/\tau_1$ ,  $\Gamma_2 = 2\hbar/\tau_2$  and  $\Gamma_\uparrow = 2\hbar/\tau_\uparrow$  (dashed line). Our calculation of the intrinsic width  $\Gamma$  for the isovector GDR in the hot nucleus  $^{112}\text{Sn}$  confirms a saturation effect in the energy dependence of  $\Gamma$ . However, we observe a systematic deviation of the evaluated width with respect to experimental values. This deviation can be reduced by varying the parameter  $x$  in Eq. (15). An increase in the parameter  $x$  improves agreement with the experiment (see dotted line in Fig. 3).

#### IV. BULK INSTABILITY

In the vicinity of the equilibrium state of the nuclear Fermi-liquid drop the stiffness coefficients for particle density and surface changes are positive and the nucleus is stable with respect to the corresponding distortions. With decreasing bulk density or increasing internal excitation energy (temperature) the liquid drop reaches regions of mechanical or



thermodynamical instabilities with respect to the small particle density and experiences shape fluctuations and separation into liquid and gas phases.

Let us consider small density fluctuations  $\delta\rho(\mathbf{r}, t)$  starting from Eq. (1). We will use a simple saturated equation of state  $\mathcal{E} \equiv \mathcal{E}[\rho] = \mathcal{E}_{kin}[\rho] + \mathcal{E}_{pot}[\rho]$  with

$$\mathcal{E}_{kin}[\rho] = \frac{\hbar^2}{2m} \left[ \frac{3}{5} \left( \frac{3\pi^2}{2} \right)^{2/3} \rho^{5/3} + \frac{1}{4} \eta \frac{(\vec{\nabla}\rho)^2}{\rho} \right], \quad (17)$$

$$\mathcal{E}_{pot}[\rho] = t_0 \rho^2 + t_3 \rho^3 + t_s (\vec{\nabla}\rho)^2 + \epsilon_C[\rho].$$

The potential energy  $\mathcal{E}_{pot}[\rho]$  has a Skyrme-type form including the surface term  $\sim (\vec{\nabla}\rho)^2$  and the Coulomb energy density,  $\epsilon_C[\rho]$ .

We will again assume a sharp surface behaviour of the equilibrium particle density. Assuming also  $\delta\rho \sim \exp(-i\omega t)$  and taking into account continuity equation and Eq. (17), the equation of motion (1) can be reduced to the following form (we consider the isoscalar mode):

$$-m\omega^2 \delta\rho = \left( \frac{1}{9} K - \frac{4}{3} \frac{i\omega\tau}{1 - i\omega\tau} (P_0/\rho_0) \right) \nabla^2 \delta\rho - 2(\beta + t_s \rho_0) \nabla^2 \nabla^2 \delta\rho, \quad (18)$$

where  $P_0 = \rho_0 p_F^2/5m$ ,  $\beta = (\hbar^2/8m)\eta$  and  $K$  is the incompressibility coefficient

$$K \approx 6\epsilon_F (1 + F_0) \quad \text{with} \quad F_0 = \frac{3\rho_0}{\epsilon_F} (t_0 + 3t_3\rho_0). \quad (19)$$

Let us consider volume instability regime,  $K < 0$ , and introduce the growth rate  $\Gamma = -i\omega$  ( $\Gamma$  is real,  $\Gamma > 0$ ). Using Eq. (18), one obtains

$$\Gamma^2 = |u_1|^2 q^2 - \zeta(\Gamma) q^2 - \kappa_s q^4, \quad (20)$$

where

$$u_1^2 = (1/9m) K, \quad \zeta(\Gamma) = \frac{4}{3m} \frac{\Gamma\tau}{1 + \Gamma\tau} \frac{P_0}{\rho_0}, \quad \kappa_s = (2/m)(\beta + t_s \rho_0). \quad (21)$$

The quantity  $\zeta(\Gamma)$  in Eq. (20) appears due to the Fermi surface distortion effect. Equation (20) is valid for arbitrary relaxation times  $\tau$  and thus describes both rare and frequent

collision limits as well as intermediate cases. From it one can obtain the leading order terms in the different limits mentioned.

(i) *Frequent collision regime:  $\tau \rightarrow 0$ . High temperatures.*

The contribution from the dynamic distortion of the Fermi surface,  $\kappa_v$ , can be neglected in this case and we have from Eqs. (20) and (4),

$$\Gamma^2 = |u_1|^2 q^2 - \Gamma (\gamma/m) q^2 - \kappa_s q^4, \quad (22)$$

where  $\gamma = (4/3)\tau P_0/\rho_0$  is the classical friction coefficient. In the limit of small friction, we obtain

$$\Gamma^2 \approx |u_1|^2 q^2 - \kappa_s q^4 - \frac{\gamma}{m} q^2 \sqrt{|u_1|^2 q^2 - \kappa_s q^4} \quad (23)$$

The amplitude of the density oscillations with a certain multipolarity  $L$ ,  $\delta\rho_L(\mathbf{r}, t)$ , grows exponentially if  $\Gamma > 0$ . The expression (23) determines two characteristic values of the wave number  $q$ , namely,  $q_{max}$  and  $q_{crit}$  where the growth rate reaches the maximum of magnitude  $\Gamma_{max}$  and  $\Gamma$  goes to zero (excluding  $q = 0$ ) respectively, i.e.,

$$\Gamma = \Gamma_{max} \text{ at } q = q_{max} < q_{crit}, \text{ and } \Gamma = 0 \text{ at } q = q_{crit}. \quad (24)$$

Both  $q_{max}$  and  $q_{crit}$  are given by

$$q_{crit}^2 = \frac{|u_1|^2}{\kappa'_s}, \quad \kappa'_s = \kappa_s + \frac{1}{m^2} \gamma^2, \quad \left. \frac{\partial \Gamma}{\partial q} \right|_{q=q_{max}} = 0. \quad (25)$$

For a saturated nuclear liquid, one has  $t_0 < 0$ ,  $t_3 > 0$  and  $t_s > 0$ . Thus, the critical value  $q_{crit}$  from Eq. (25) increases with a decrease of the bulk density  $\rho_0$ , see Eqs. (19) and (25). The presence of friction decreases the critical value  $q_{crit}$ , i.e. reduces the instability. The existence of the critical wave number  $q_{crit}$  for an unstable mode is a feature of a finite system. The growth rate  $\Gamma$  depends on the multipolarity  $L$  of the nuclear density distortion and on the position of  $q_L$  in the interval  $q = 0 \div q_{crit}$  [13]. The value of  $q_L$  is determined from the boundary condition for the pressure on free nuclear surface. For given  $R_0$  the value of  $q_L$  increases with  $L$  at  $L \geq 2$ . That means that if  $q_L < q_{max}$  instability increases with

$L$  and the nucleus becomes more unstable with respect to internal clusterization into small pieces (high multipolarity or multifragmentation regimes) rather than to binary fission (low multipolarity regime). In contrast, the binary fission is preferable if  $q_{max} < q_L < q_{crit}$ .

(ii) *Rare collision regime:  $\tau \rightarrow \infty$ . Cold expansion.*

Neglecting the contribution from the relaxation, one has from Eq. (20)

$$\Gamma^2 = |u_1|^2 q^2 - \kappa'_v q^2 - \kappa_s q^4, \quad \kappa'_v = \frac{4}{3} \frac{P_{eq}}{m \rho_{eq}}. \quad (26)$$

The critical value  $q_{crit}$  and the value  $q_{max}$  are given by

$$q_{crit}^2 = \frac{|u_1|^2 - \kappa'_v}{\kappa_s}, \quad q_{max}^2 = \frac{1}{2} q_{crit}^2. \quad (27)$$

Thus, the distortion of the Fermi-surface leads to a decrease of the critical value  $q_{crit}$  i.e. the Fermi-liquid drop becomes more stable with respect to volume density fluctuations due to dynamic Fermi-surface distortion effects.

## REFERENCES

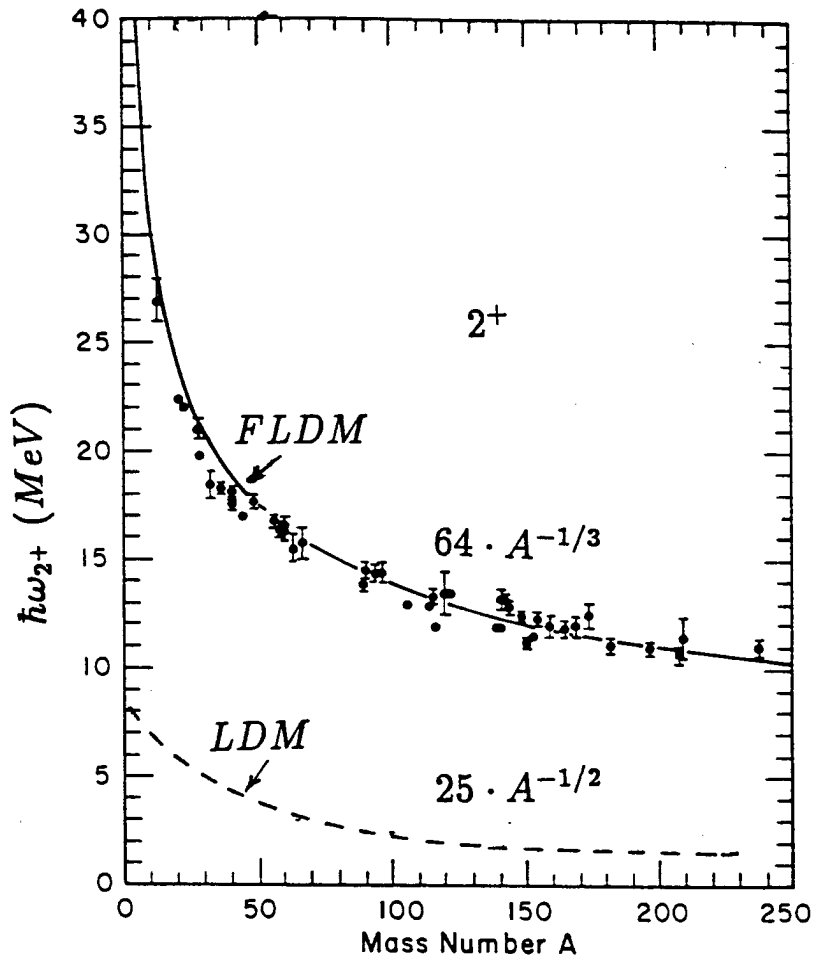
- [1] A.A. Abrikosov and I.M. Khalatnikov, *Rep. Prog. Phys.* **22**, 329 (1959).
- [2] V.M. Kolomietz and H.H.K. Tang, *Phys. Scripta* **24**, 915 (1981).
- [3] V.M. Kolomietz, *Local Density Approach for Atomic and Nuclear Physics* (Naukova Dumka, Kiev, 1990) (in Russian).
- [4] G. Holzwarth and G. Eckart, *Nucl. Phys.* **A325**, 1 (1979).
- [5] V.M. Kolomietz, V.A. Plujko and S. Shlomo, *Phys. Rev. C* **52**, 2480 (1995).
- [6] A. Bohr and B.R. Mottelson, *Nuclear Structure, Volume II* (Benjamin, New York, 1975).
- [7] V.M. Kolomietz, A.G. Magner and V.A. Plujko, *Z. Phys.* **A345**, 131, 137 (1993).
- [8] J.P. Blaizot and B. Grammaticos, *Nucl. Phys.* **A355**, 115 (1981).
- [9] K. Sato and S. Yoshida, *Phys. Rev. C* **52**, 837 (1995).
- [10] V.M. Kolomietz, V.A. Plujko and S. Shlomo, *Phys. Rev. C* **54**, 3014 (1996).
- [11] V.M. Kolomietz, S.V. Lukyanov, V.A. Plujko and S. Shlomo, *Phys. Rev. C* **58**, # 1 (1998).
- [12] K. Ando, A. Ikeda and G. Holzwarth, *Z. Phys.* **A310**, 223 (1983).
- [13] C.J. Pethick and D.G. Ravenhall, *Nucl. Phys.* **A471**, 19c (1987).
- [14] D. Kiderlen, V.M. Kolomietz and S. Shlomo, *Nucl. Phys.* **A608**, 32 (1996).
- [15] F.E. Bertrand, *Nucl. Phys.* **A354**, 129c (1981).
- [16] J. J. Gaardhoje, *Ann. Rev. Nucl. Part. Sci.* **42**, 483 (1992).

## FIGURES

FIG. 1. Energies of the lowest isoscalar  $2^+$  excitations as evaluated in the traditional liquid drop model [6] (LDM), i.e., at  $C'(\omega) = 0$  and in the Fermi-liquid drop model (FLDM) taking into account both contributions  $C^{(LD)}$  and  $C'(\omega)$  in Eq. (2). The experimental data are from Ref. [15].

FIG. 2. Energies of the isoscalar monopole resonances in the liquid drop model (dashed line) and in the Fermi-liquid drop model (solid line). Experimental data from Ref. [15].

FIG. 3. The intrinsic width of the isovector giant dipole resonance in the nucleus  $^{112}\text{Sn}$  as function of excitation energy  $U$ . The experimental data were taken from Ref. [16]. Solid line corresponds to the total width. Dashed line is the width in the zero sound approximation at  $\Gamma = 2\hbar/\tau$ . Dotted line is the fit to the experimental data due to the parameter  $x = 0.78$  in Eq. (15), see Ref. [5].



# ISOSCALAR MONOPOLE RESONANCE

